Continuum Mech. Thermodyn. 4 (1992) 279–312

Continuum Mechanics and Thermodynamics

Mathematical analysis of a two-phase continuum mixture theory

P. Embid and **M. Baer**

In this paper, we study the mathematical structure of a continuum reactive mixture model of the combustion of granular energetic materials. We obtain and classify the wave fields associated with this description. This analysis shows that this system of hyperbolic equations becomes degenerate when the relative flow is locally sonic. We derive the corresponding Riemann invariants and construct simple wave solutions. We also discuss special discontinuous solutions of the system of equations. For fixed upstream conditions, different downstream states are possible when the relative velocities exceed the speed of the sound gas.

List of symbols

a	s (solid), g (gas) subscript to indicate the phase
v_a	velocity of phase a
v_{sg}	$v_s - v_g$
ρ_a	material density
V_a	specific volume
p_a	pressure
T_a	temperature
e_a	internal energy
η_a	entropy
h_a	enthalpy $= e_a + p_a/\rho_a$
ψ_a	Helmholtz free energy $= e_a - T_a\eta_a$
ϕ_a	volume fraction
β_a	configuration pressure $= \phi_a\rho_a \left(\dfrac{\partial\psi_a}{\partial\phi_a}\right)_{\rho_a, T_a}$

c_a speed of sound $= \left(\frac{\partial p_a}{\partial \rho_a}\right)^{1/2}_{\eta_a, \phi_a}$

Γ_a Grüneisen coefficient $= \frac{1}{\rho_a}\left(\frac{\partial p_a}{\partial e_a}\right)_{\rho_a, \phi_a}$

$C_a^\dagger$ rate of mass production
$m_a^\dagger$ rate of momentum production
$e_a^\dagger$ rate of energy production
δ drag coefficient
h heat transfer coefficient
k_a thermal conductivity
μ_c compaction viscosity
F $\phi_s \phi_g [p_s - p_g - \beta_s]/\mu_c$

1 Introduction

To describe the combustion behavior of granular energetic materials, such as explosive powders, the chemical/thermal/mechanical behavior of a mixture of phases must be treated. Much of the foundations of current modeling have been based on the ideas and methods of modern continuum mechanics (as set forth, for example, by Truesdell and Toupin [1], and Truesdell and Noll [2]), and in particular on the assumption that all phases are superposed (e.g., Truesdell and Toupin, § 157). Unfortunately, the formulation and development of conservation laws governing reactive multiphase flow are not universally accepted, and a certain level of controversy remains in the multiphase flow literature. Much of this controversy stems from the use of various averaging methods to bypass the discrete nature of the phases. (A review of relevant literature for reactive multiphase flow can be found in reference [3].)

In continuum mixture models, conservation laws are assumed for each phase and constitutive relations account for the exchange of mass, momentum, and energy between phases. Overall conservation of mass, momentum and energy is also required for the total mixture which results in constraints on the interaction between the phases. The mathematical structure of these descriptions has not been adequately studied in the past – indeed, multiphase flow models have been proposed that are now recognized to be ill-conditioned [4, 5, 6].

Guided by the foundation of continuum mixture theory and experimental observation, Baer and Nunziato [3] developed a model for the flame spread and growth to detonation in granular materials. Their model treats each phase as fully compressible and in thermodynamic nonequilibrium. The problem of closure, required to produce a formally determined system of equations, is resolved using the entropy inequality (see [3] for details). An evolution equation for the solid volume fraction is developed to describe compaction of the solid phase. In this approach, rate-dependent compaction and compressibility

of all phases are consistently treated. Additionally, the use of unequal phase pressures and intragranular stress removes the mathematical ill-posed nature of the equations known to exist in equal pressure multiphase flow models. Numerical experiments and comparison with experimental data have provided validation of the model. The purpose of this work is to investigate the mathematical structure of this continuum mixture model. Beyond investigating the implication of modeling assumptions, the wave characteristics are established as a guide for a characteristic-based numerical scheme.

We organized this paper as follows. Section 2 introduces the model, which, in the absence of diffusive effects, is represented by a 7×7 hyperbolic system. This system is not strictly hyperbolic, and cannot be completely cast into divergence form. We find the associated eigenvalues and eigenvectors and show that the system becomes degenerate at points where the flow is *choked.* The different wave fields are then classified. In Section 3, *simple wave* solutions are determined for the system when the source terms are ignored. For the construction of such solutions, we derive the associated *generalized Riemann invariants.* In Section 4 we construct *centered rarefaction waves* and *contact discontinuities.* Finally, in Section 5 the jump conditions for the equations in conservation form are discussed and used to determine special discontinuous solutions and to show that under certain upstream and downstream conditions there exist multiple discontinuous solutions of the equations. One of the solutions is a contact discontinuity in the solid phase and the other solution is a shock. Interestingly, these multiple jump states arise when the relative gas velocity exceeds the sound speed of the gas. These solutions satisfy both the entropy condition and Lax's geometric shock condition. Clearly, a more detailed study of the mathematical character of the multiphase reactive flow equations is warranted, and future studies may lead to a better understanding of the coupling of the various modes of combustion.

2 Characteristic analysis of the continuum multiphase model

In describing chemically reactive two-phase mixtures, we treat a flow consisting of a solid reactant (s) and an interstitial gas (g). In the theory developed by Baer and Nunziato [3], field equations are formulated expressing the conservation of mass, momentum and energy for each phase (including transfer effects between the phases), and appropriate mixture constraints are imposed to preserve conservation conditions for the total mixture. The interested reader is referred to reference [3] for the complete derivation of the continuum multiphase flow model. Following the formal derivation of the balance equations given in [1], the field equations governing the combustion of granular energetic mixtures obtained in [3] are (for the meaning of the variables check the list of symbols):

Conservation of mass

$$\frac{\partial \rho_s}{\partial t} + v_s \frac{\partial \rho_s}{\partial x} = -\rho_s \frac{\partial v_s}{\partial x} - \frac{\rho_s}{\phi_s} F \tag{2.1}$$

$$\frac{\partial \rho_g}{\partial t} + v_g \frac{\partial \rho_g}{\partial x} = -\rho_g \frac{\partial v_g}{\partial x} - \frac{\rho_g}{\phi_g}(v_s - v_g)\frac{\partial \phi_s}{\partial x} + \frac{\rho_g}{\phi_g} F - \left(1 - \frac{\rho_g}{\rho_s}\right)\frac{C_s^\dagger}{\phi_g} \tag{2.2}$$

Conservation of momentum

$$\phi_s \rho_s \left[\frac{\partial v_s}{\partial t} + v_s \frac{\partial v_s}{\partial x}\right] = -\phi_s \frac{\partial p_s}{\partial x} + (p_g - p_s)\frac{\partial \phi_s}{\partial x} - \left(\delta + \frac{C_s^\dagger}{2}\right)(v_s - v_g) \tag{2.3}$$

$$\phi_g \rho_g \left[\frac{\partial v_g}{\partial t} + v_g \frac{\partial v_g}{\partial x}\right] = -\phi_g \frac{\partial p_g}{\partial x} + \left(\delta + \frac{C_s^\dagger}{2}\right)(v_s - v_g) \tag{2.4}$$

Conservation of energy

$$\phi_s \rho_s \left[\frac{\partial e_s}{\partial t} + v_s \frac{\partial e_s}{\partial x}\right] = -\phi_s p_s \frac{\partial v_s}{\partial x} + \frac{\partial}{\partial x}\left(k_s \frac{\partial T_s}{\partial x}\right) \tag{2.5}$$

$$-h(T_s - T_g) - (p_s - \beta_s) F$$

$$\phi_g \rho_g \left[\frac{\partial e_g}{\partial t} + v_g \frac{\partial e_g}{\partial x}\right] = -\phi_g p_g \frac{\partial v_g}{\partial x} + \frac{\partial}{\partial x}\left(k_g \frac{\partial T_g}{\partial x}\right)$$

$$+h(T_s - T_g) + (p_s - \beta_s) F - (v_s - v_g) p_g \frac{\partial \phi_s}{\partial x}$$

$$+ \delta(v_s - v_g)^2 - (e_s - e_g) C_s^\dagger \tag{2.6}$$

Solid volume fraction

$$\frac{\partial \phi_s}{\partial t} + v_s \frac{\partial \phi_s}{\partial x} = F + \frac{C_s^\dagger}{\rho_s}. \tag{2.7}$$

Closure for the system is given by the saturation constraint

$$\phi_g = 1 - \phi_s, \tag{2.8}$$

and the equations of state for each phase

$$p_a = p_a(\rho_a, e_a). \tag{2.9}$$

Equations (2.1)–(2.8) correspond to equations (53)–(60) in [3]. However, we remark that in [3] the solid volume fraction is denoted by α_s, and the partial density by ρ_a, whereas here the solid volume fraction is given by ϕ_s, the partial density by $\phi_a\rho_a$, and ρ_a stands for the material density. The thermodynamic relationship for the Helmholtz free energy of each phase satisfies the differential relation:

$$d\psi_a = -\eta_a dT_a + \frac{p_a}{\rho_a^2} d\rho_a + \frac{\beta_a}{\phi_a\rho_a} d\phi_a, \tag{2.10}$$

and for the gas variable it is assumed [3] that the configuration pressure $\beta_g = 0$. Using (2.9) and (2.10) yields the following differential relations for the energy and the pressure

$$\begin{aligned} de_a &= T_a d\eta_a + \frac{p_a}{\rho_a^2} d\rho_a + \frac{\beta_a}{\phi_a\rho_a} d\phi_a, \\ dp_a &= \rho_a \Gamma_a T_a d\eta_a + c_a^2 d\rho_a + \frac{\Gamma_a \beta_a}{\phi_a} d\phi_a. \end{aligned} \tag{2.11}$$

Using equations (2.10) and (2.11) we recast the multiphase flow equations (2.1)–(2.7) as a 7×7 system

$$\frac{\partial \mathbf{U}}{\partial t} + \mathbf{A}(\mathbf{U}) \frac{\partial \mathbf{U}}{\partial x} = \mathbf{S}(\mathbf{U}), \tag{2.12}$$

where the vector $\mathbf{U}$ of states variables is given by

$$\mathbf{U} = (\rho_s, v_s, \eta_s, \phi_s, \rho_g, v_g, \eta_g)^T. \tag{2.13}$$

Hereafter we reserve the boldface notation for vectors and matrices. In addition, the superscript T stands for transpose and emphasizes that $\mathbf{U}$ is a column vector. $\mathbf{A}(\mathbf{U})$ is the 7×7 matrix

$$\begin{pmatrix} v_s & \rho_s & 0 & 0 & 0 & 0 & 0 \\ c_s^2/\rho_s & v_s & \Gamma_s T_s & (p_s - p_g + \Gamma_s\beta_s)/(\phi_s\rho_s) & 0 & 0 & 0 \\ 0 & 0 & v_s & 0 & 0 & 0 & 0 \\ 0 & 0 & 0 & v_s & 0 & 0 & 0 \\ 0 & 0 & 0 & \rho_g(v_s - v_g)/\phi_g & v_g & \rho_g & 0 \\ 0 & 0 & 0 & 0 & c_g^2/\rho_g & v_g & \Gamma_g T_g \\ 0 & 0 & 0 & 0 & 0 & 0 & v_g \end{pmatrix}, \tag{2.14}$$

and the source vector $\mathbf{S}(\mathbf{U})$ is given by

$$\begin{pmatrix} -\frac{\rho_s}{\phi_s} F \\ -\frac{1}{\phi_s \rho_s}\left(\delta + \frac{C_s^\dagger}{2}\right)(v_s - v_g) \\ \frac{1}{\phi_s \rho_s T_s}\left\{\frac{\partial}{\partial x}\left(k_s \frac{\partial T_s}{\partial x}\right) - h(T_s - T_g) - \frac{\beta_s}{\rho_s} C_s^\dagger\right\} \\ F + \frac{C_s^\dagger}{\rho_s} \\ \frac{\rho_g}{\phi_g} F - \left(1 - \frac{\rho_g}{\rho_s}\right)\frac{C_s^\dagger}{\phi_g} \\ \frac{1}{\phi_g \rho_g}\left(\delta - \frac{C_s^\dagger}{2}\right)(v_s - v_g) \\ \frac{1}{\phi_g \rho_g T_g}\left\{\frac{\partial}{\partial x}\left(k_g \frac{\partial T_g}{\partial x}\right) + h(T_s - T_g) + \delta(v_s - v_g)^2 \right. \\ \left. + (p_s - p_g - \beta_s) F + \left[e_g - e_s + \left(\frac{1}{\rho_s} - \frac{1}{\rho_g}\right) p_g\right] C_s^\dagger\right\} \end{pmatrix}. \tag{2.15}$$

For the characteristics analysis, one works with the homogeneous form of (2.12). Thus, we set $\mathbf{S}(\mathbf{U}) \equiv 0$ and consider the system

$$\frac{\partial \mathbf{U}}{\partial t} + \mathbf{A}(\mathbf{U}) \frac{\partial \mathbf{U}}{\partial x} = 0. \tag{2.16}$$

The mathematical structure of the system is more clearly revealed and the characteristics analysis given below is simplified if $\mathbf{U}$ and $\mathbf{A}(\mathbf{U})$ are partitioned into blocks representing the state variables for the solid, the gas, and the solid volume fraction such that

$$\begin{aligned} &\mathbf{U} = (\mathbf{U}_s | \phi_s | \mathbf{U}_g)^T, \\ &\mathbf{U}_a = (\rho_a, v_a, \eta_a)^T, \quad a = s, g, \end{aligned} \tag{2.17}$$

and the matrix $\mathbf{A}(\mathbf{U})$ has the block structure

$$\mathbf{A}(\mathbf{U}) = \left(\begin{array}{c|c|c} \mathbf{A}_s & * & 0 \\ \hline 0 & v_s & 0 \\ \hline 0 & * & \mathbf{A}_g \end{array}\right), \tag{2.18}$$

where,

$$\mathbf{A}_a = \begin{pmatrix} v_a & \rho_a & 0 \\ c_a^2/\rho_a & v_a & \Gamma_a T_a \\ 0 & 0 & v_a \end{pmatrix}.$$

The special structure of the matrix $\mathbf{A}(\mathbf{U})$ in (2.18) makes it relatively easy to carry out the characteristics analysis for the system. $\mathbf{A}(\mathbf{U})$ consists of two 3×3 block matrices $\mathbf{A}_a$ that correspond precisely to one-phase gas dynamics for the a-phase in the variables ρ_a, v_a, and η_a, coupled through the solid volume fraction terms. Since we know the wave speeds for ordinary gas dynamics, the eigenvalues of the two-phase system are immediately determined; expanding $\det(\mathbf{A}(\mathbf{U}) - \lambda\mathbf{I})$ along the fourth row gives

$$0 = \det(\mathbf{A}(\mathbf{U}) - \lambda\mathbf{I}) = (v_s - \lambda) \prod_{a=s,g} \det(\mathbf{A}_a(\mathbf{U}_a) - \lambda\mathbf{I})$$

$$= (v_s - \lambda) \prod_{a=s,g} (v_a - \lambda)[(v_a - \lambda)^2 - c_a^2],$$

and this yields the

Eigenvalues of A(U)

$$\begin{aligned} &\lambda_s^- = v_s - c_s, \quad \lambda_s^+ = v_s + c_s, \quad \lambda_s^0 = v_s, \quad \lambda_s^c = v_s, \\ &\lambda_g^- = v_g - c_g, \quad \lambda_g^+ = v_g + c_g, \quad \lambda_g^0 = v_g. \end{aligned} \tag{2.19}$$

These eigenvalues give the familiar forward and backward acoustic speeds and the particle speeds for the solid and the gas. Since all the eigenvalues, i.e. wave speeds, are real, this system does not produce unphysical instabilities as other multiphase flow models such as the pressure equilibrium model [4, 5, 6]. The particle speed v_s of the solid is a repeated eigenvalue and it is associated with two modes of propagation corresponding to entropy waves and compaction waves for the solid; this is clear because the compaction equation (2.7) for the solid volume fraction is already in characteristic form, with characteristic speed v_s. Because of the block structure of $\mathbf{A}(\mathbf{U})$, the associated right eigenvectors are immediately given by those from one-phase gas dynamics, with the exception of the one associated with the compaction mode $\lambda = v_s$, which is computed separately:

Right Eigenvectors of A(U)

$$\mathbf{r}_s^- = \left(1, -\frac{c_s}{\rho_s}, 0, 0, 0, 0, 0\right)^T,$$

$$\mathbf{r}_s^+ = \left(1, \frac{c_s}{\rho_s}, 0, 0, 0, 0, 0\right)^T,$$

$$\mathbf{r}_s^0 = \left(1, 0, -\frac{c_s^2}{\rho_s \Gamma_s T_s}, 0, 0, 0, 0\right)^T,$$

$$\mathbf{r}_s^c = \left(0, 0, -\frac{(p_s - p_g + \Gamma_s \beta_s)}{\phi_s \rho_s \Gamma_s T_s}, 1, \frac{\rho_g (v_s - v_g)^2}{\phi_g [(v_s - v_g)^2 - c_g^2]},\right.$$
$$\left.\frac{c_g^2 (v_s - v_g)}{\phi_g [(v_s - v_g)^2 - c_g^2]}, 0\right)^T, \tag{2.20}$$

$$\mathbf{r}_g^- = \left(0, 0, 0, 0, 1, -\frac{c_g}{\rho_g}, 0\right)^T,$$

$$\mathbf{r}_g^+ = \left(0, 0, 0, 0, 1, \frac{c_g}{\rho_g}, 0\right)^T,$$

$$\mathbf{r}_g^0 = \left(0, 0, 0, 0, 1, 0, -\frac{c_g^2}{\rho_g \Gamma_g T_g}\right)^T.$$

The system is not strictly hyperbolic because v_s is a double eigenvalue, and also because the wave speeds associated with the different phases change independently of each other, so that the eigenvalues of the solid phase can coincide with any of those of the gas phase. States where the system is not strictly hyperbolic occur when (a) $v_s = v_g$, (b) $v_s = v_g \pm c_g$, (c) $v_g = v_s \pm c_s$, and (d) $v_s \pm c_s = v_g \pm c_g$. Some of these conditions are more likely to occur than others. For example, (a) occurs in flows starting from rest, where initially $v_s = v_g = 0$. The conditions given in (c) and (d) can occur for detonation states in condensed phases; however, we consider flows where c_s is much larger than v_s, v_g, and c_g. A very interesting condition corresponds to (b) where the relative flow is locally sonic. We also remark that our analysis assumes the existence of two phases, so that ϕ_s and ϕ_g are both non zero. We are not considering the extreme case where one of the phases disappears and the multiphase flow system becomes highly degenerate. Although the system is not strictly hyperbolic, it is totally hyperbolic provided that the right eigenvectors constitute a basis. Inspection of the eigenvectors in (2.20) shows that the system is totally hyperbolic except in case (b) where $v_g \pm c_g = v_s$. In this case v_s becomes a triple eigenvalue with only two independent eigenvectors because the compaction eigenvector (suitably scaled) degenerates into the gas acoustic eigenvector:

$$\lim_{v_s - v_g \to \pm c_g} \frac{\phi_g}{\rho_g c_g^2} [(v_s - v_g)^2 - c_g^2] \mathbf{r}_s^c = \mathbf{r}_g^{\pm}. \tag{2.21}$$

We term $v_s - v_g = \pm c_g$ the *chocked flow condition.* As a physical interpretation, flow at the pore level is analogous to the flow in a moving duct with a variable cross-section area (due to local variations of volume fraction).

Consistent with this duct flow analogy, a choked flow is reached when the relative velocity is sonic, or $|v_s - v_g| = c_g$.

Mathematically, when the set of eigenvectors is not complete but the eigenvalues of **A** are still real, a parabolic degeneracy exists. In this case the Jordan form of **A(U)** has a nontrivial block. This is exactly the situation when $v_s = v_g \pm c_g$; v_s becomes a triple eigenvalue with only two associated right eigenvectors $\mathbf{r}_s^0$, and $\mathbf{r}_g^{\pm}$, and one generalized eigenvector $\mathbf{r}_*$ obtained by solving

$$(\mathbf{A} - \lambda \mathbf{I})\, \mathbf{r}_* = \mathbf{r}_g^{\pm}. \tag{2.22}$$

The eigenvector $\mathbf{r}_*$ is given explicitly as

$$\mathbf{r}_* = \left(0, 0, \mp \frac{2\phi_g}{\rho_g c_g} \frac{(p_s - p_g + \Gamma_s \beta_s)}{\phi_s \rho_s \Gamma_s T_s}, \pm \frac{2\phi_g}{\rho_g c_g}, \pm \frac{1}{c_g}, 0, 0\right)^T.$$

The coupling present in (2.22) suggests the possibility that strong resonant interactions of the gas acoustic and the compaction mode can occur near choked flow conditions. Based on the characteristics analysis presented here, Embid et al. [7] derived an asymptotic model for the transition to detonation in reactive granular flows in regimes near choked flow and ignition temperature conditions, and Embid and Majda [8] analyzed the asymptotic model, and showed how it can qualitatively predict the formation of hot spots and the transition to detonation in various interesting regimes previously documented [3, 9, 10]. We also remark that these choked flow singularities of the two-phase flow model do not have a counterpart in one-phase flows.

We finish this section with the construction of the left eigenvectors and the recasting of the system (2.1)–(2.7) into characteristic form. The left eigenvectors $\mathbf{l}_j$ of the matrix **A(U)** are defined as the basis dual to the basis of right eigenvectors $\mathbf{r}_i$, $i,j = 1, \ldots, 7$, i.e.

$$\mathbf{l}_j \cdot \mathbf{r}_i = \delta_{ij} \quad i,j = 1, \ldots, 7. \tag{2.23}$$

Except at choked flow points, the right eigenvectors given in (2.20) are a basis; in this case (2.20) and (2.23) give the

Left Eigenvectors of A(U)

$$\mathbf{l}_s^- = \left(\frac{1}{2}, -\frac{\rho_s}{2c_s}, \frac{\rho_s \Gamma_s T_s}{2c_s^2}, \frac{p_s - p_g + \Gamma_s \beta_s}{2\phi_s c_s^2}, 0, 0, 0\right),$$

$$\mathbf{l}_s^0 = \left(0, 0, -\frac{\rho_s \Gamma_s T_s}{c_s^2}, -\frac{p_s - p_g + \Gamma_s \beta_s}{\phi_s c_s^2}, 0, 0, 0\right),$$

$$\mathbf{l}_s^+ = \left(\frac{1}{2}, \frac{\rho_s}{2c_s}, \frac{\rho_s \Gamma_s T_s}{2c_s^2}, \frac{p_s - p_g + \Gamma_s \beta_s}{2\phi_s c_s^2}, 0, 0, 0\right),$$

$$\mathbf{l}_s^c = (0, 0, 0, 1, 0, 0, 0), \tag{2.24}$$

$$\mathbf{l}_g^- = \left(0, 0, 0, -\frac{\rho_g(v_s - v_g)}{2\phi_g(v_s - v_g + c_g)}, \frac{1}{2}, -\frac{\rho_g}{2c_g}, \frac{\rho_g \Gamma_g T_g}{2c_g^2}\right),$$

$$\mathbf{l}_g^0 = \left(0, 0, 0, 0, 0, 0, -\frac{\rho_g \Gamma_g T_g}{c_g^2}\right),$$

$$\mathbf{l}_g^+ = \left(0, 0, 0, -\frac{\rho_g(v_s - v_g)}{2\phi_g(v_s - v_g - c_g)}, \frac{1}{2}, \frac{\rho_g}{2c_g}, \frac{\rho_g \Gamma_g T_g}{2c_g^2}\right).$$

Finally, we derive the characteristic form of the multiphase flow equations. Taking the product of equation (2.12) with the left eigenvector $\mathbf{l}_i$ associated with the eigenvalue λ_i produces

$$\mathbf{l}_i \mathbf{S}(\mathbf{U}) = \mathbf{l}_i \left(\frac{\partial \mathbf{U}}{\partial t} + \mathbf{A}\frac{\partial \mathbf{U}}{\partial x}\right) = \mathbf{l}_i \left(\frac{\partial \mathbf{U}}{\partial t} + \lambda_i \frac{\partial \mathbf{U}}{\partial x}\right), \quad i = 1, \ldots, 7. \tag{2.25}$$

This set of equations represents the characteristic form of (2.12). It gives algebraic relations for the rates of change of the state variables along the *ith - characteristic* moving at speed λ_i. For the multiphase flow equations they are given explicitly by

Solid Acoustics $(\lambda = v_s \pm c_s)$

$$\phi_s c_s^2 \left[\frac{\partial \rho_s}{\partial t} + (v_s \pm c_s)\frac{\partial \rho_s}{\partial x}\right] \pm \phi_s \rho_s c_s \left[\frac{\partial v_s}{\partial t} + (v_s \pm c_s)\frac{\partial v_s}{\partial x}\right]$$

$$+ \phi_s \rho_s \Gamma_s T_s \left[\frac{\partial \eta_s}{\partial t} + (v_s \pm c_s)\frac{\partial \eta_s}{\partial x}\right] + (p_s - p_g + \Gamma_s \beta_s)\left[\frac{\partial \phi_s}{\partial t} + (v_s \pm c_s)\frac{\partial \phi_s}{\partial x}\right]$$

$$= (p_s - p_g + \Gamma_s \beta_s - \rho_s c_s^2) F + \left[\mp \frac{c_s}{2}(v_s - v_g) + \frac{p_s - p_g}{\rho_s}\right] C_s^\dagger \mp c_s(v_s - v_g)\,\delta$$

$$+ \Gamma_s \frac{\partial}{\partial x}\left(k_s \frac{\partial T_s}{\partial x}\right) - \Gamma_s(T_s - T_g)\,h. \tag{2.26}$$

Solid Entropy $(\lambda = v_s, \mathbf{l} = \mathbf{l}_s^0)$

$$\frac{\partial \eta_s}{\partial t} + v_s \frac{\partial \eta_s}{\partial x} = \frac{1}{\phi_s \rho_s T_s}\left\{\frac{\partial}{\partial x}\left(k_s \frac{\partial T_s}{\partial x}\right) - h(T_s - T_g) - \frac{\beta_s}{\rho_s} C_s^\dagger\right\}. \tag{2.27}$$

Compaction Equation $(\lambda = v_s, \mathbf{l} = \mathbf{l}_0^c)$

$$\frac{\partial \phi_s}{\partial t} + v_s \frac{\partial \phi_s}{\partial x} = F + \frac{C_s^\dagger}{\rho_s}. \tag{2.28}$$

Gas Acoustics $(\lambda = v_g \pm c_g)$

$$\phi_g c_g^2 \left[\frac{\partial \rho_g}{\partial t} + (v_g \pm c_g)\frac{\partial \rho_g}{\partial x}\right] \pm \phi_g \rho_g c_g \left[\frac{\partial v_g}{\partial t} + (v_g \pm c_g)\frac{\partial v_g}{\partial x}\right]$$

$$+ \phi_g \rho_g \Gamma_g T_g \left[\frac{\partial \eta_g}{\partial t} + (v_g \pm c_g)\frac{\partial \eta_g}{\partial x}\right] - \frac{\rho_g c_g^2 (v_s - v_g)}{(v_s - v_g \mp c_g)} \left[\frac{\partial \phi_s}{\partial t} + (v_g \pm c_g)\frac{\partial \phi_s}{\partial x}\right]$$

$$= \left[\mp \frac{\rho_g c_g^3}{(v_s - v_g \mp c_g)} + \Gamma_g (p_s - p_g - \beta_s)\right] F$$

$$+ \Gamma_g \frac{\partial}{\partial x}\left(k_g \frac{\partial T_g}{\partial x}\right) + [\pm c_g (v_s - v_g) + \Gamma_g (v_s - v_g)^2]\,\delta \tag{2.29}$$

$$+ \left[-c_g^2 \mp \frac{\rho_g c_g^3}{\rho_s (v_s - v_g \mp c_g)} \mp c_g \frac{(v_s - v_g)}{2} + \Gamma_g (e_g - e_s)\right.$$

$$\left. + \Gamma_g p_g \left(\frac{1}{\rho_s} - \frac{1}{\rho_g}\right)\right] C_s^\dagger + h\Gamma_g (T_s - T_g).$$

Gas Entropy $(\lambda = v_g)$

$$\frac{\partial \eta_g}{\partial t} + v_g \frac{\partial \eta_g}{\partial x} = \frac{1}{\phi_g \rho_g T_g}\left\{\frac{\partial}{\partial x}\left(k_g \frac{\partial T_g}{\partial x}\right) + h(T_s - T_g)\right.$$

$$+ \delta (v_s - v_g)^2 + (p_s - p_g - \beta_s) F \tag{2.30}$$

$$\left. + \left[e_g - e_s + \left(\frac{1}{\rho_s} - \frac{1}{\rho_g}\right) p_g\right] C_s^\dagger\right\}.$$

Having established formally this mathematical foundation, sufficient framework has been laid for constructing a numerical method based on the characteristics. Many modern computational methods use embedded Riemann solvers (or approximate Riemann solutions) in algorithms to enhance accuracy of numerical solution. In the next section, we provide the necessary ingredients for such a method.

3 Simple waves, classification of wave fields and generalized Riemann invariants

Consider a linear, constant coefficient hyperbolic system of the form

$$\frac{\partial \mathbf{U}}{\partial t} + \mathbf{A}\frac{\partial \mathbf{U}}{\partial x} = 0,$$

where $\mathbf{A}$ has real eigenvalues $\lambda_1 \leqq \lambda_2 \ldots \leqq \lambda_n$ and a corresponding basis of right eigenvectors $\{\mathbf{r}_1, \mathbf{r}_2, \ldots, \mathbf{r}_n\}$. The normal mode solutions of this system are defined by

$$\mathbf{U}_k(x,t) = \sigma_k(x,t)\,\mathbf{r}_k; \quad k = 1, \ldots, n,$$

where the scalar function $\sigma_k(x,t)$ is a solution of the equation

$$\frac{\partial \sigma_k}{\partial t} + \lambda_k \frac{\partial \sigma_k}{\partial x} = 0.$$

Now consider a nonlinear system of the form

$$\frac{\partial \mathbf{U}}{\partial t} + \mathbf{A}(\mathbf{U}) \frac{\partial \mathbf{U}}{\partial x} = 0, \tag{3.1}$$

where $\mathbf{A}(\mathbf{U})$ has real eigenvalues $\lambda_1(\mathbf{U}), \ldots, \lambda_n(\mathbf{U})$ and a corresponding basis of right eigenvectors $\{\mathbf{r}_1(\mathbf{U}), \ldots, \mathbf{r}_n(\mathbf{U})\}$. There exist special smooth solutions of (3.1), analogous to the normal mode solutions for the linear case. They are called *simple waves* and are given by [11]:

$$\mathbf{U}_k(x,t) = \mathbf{U}_k(\sigma_k(x,t)), \tag{3.2}$$

where $\mathbf{U}_k(\sigma)$ is now a curve everywhere tangent to the vector field $\mathbf{r}_k(\mathbf{U})$, so that $\mathbf{U}_k(\sigma)$ solves the ODE system

$$\frac{d\mathbf{U}_k}{d\sigma} = \mathbf{r}_k(\mathbf{U}_k(\sigma)) \quad \text{on } \sigma_1 < \sigma < \sigma_2, \tag{3.3}$$

$$\mathbf{U}_k(\sigma_0) = \mathbf{U}_{k0}, \quad \sigma_1 < \sigma_0 < \sigma_2,$$

and the amplitude $\sigma_k(x,t)$ is a solution of the scalar PDE

$$\frac{\partial \sigma_k}{\partial t} + \lambda_k(\mathbf{U}_k(\sigma_k(x,t))) \frac{\partial \sigma_k}{\partial x} = 0, \tag{3.4}$$

$$\sigma_k(x,0) = \sigma_{k0}(x), \quad \sigma_1 < \sigma_{k0}(x) < \sigma_2.$$

These solutions will exhibit nonlinear behavior if the speed of propagation $\lambda_k(\mathbf{U}_k(\sigma))$ is a function of the amplitude σ_k, i.e. if

$$0 \neq \frac{d}{d\sigma}\{\lambda_k(\mathbf{U}_k(\sigma))\} = \nabla\lambda_k(\mathbf{U}_k(\sigma)) \cdot \mathbf{r}_k(\mathbf{U}_k(\sigma)).$$

Alternatively, the solutions exhibit linear behavior when their speed of propagation is constant

$$0 \equiv \frac{d}{d\sigma}\{\lambda_k(\mathbf{U}_k(\sigma))\} = \nabla\lambda_k(\mathbf{U}_k(\sigma)) \cdot \mathbf{r}_k(\mathbf{U}_k(\sigma)).$$

Lax [12] classified the wave field associated with $\lambda_k(\mathbf{U})$ as *genuinely nonlinear* if

$$\nabla\lambda_k(\mathbf{U}) \cdot \mathbf{r}_k(\mathbf{U}) \neq 0,$$

for all **U**, and *linearly degenerate* if

$$\nabla\lambda_k(\mathbf{U})\cdot\mathbf{r}_k(\mathbf{U})\equiv 0,$$

for all **U**. For the multiphase flow system we will see that under standard convexity conditions for the equations of state of both phases, analogous to the ones given for gas dynamics [13], the acoustic modes are genuinely nonlinear, and the entropy modes are linearly degenerate just as for one-phase flows [11, 12, 14]; also the compaction mode is linearly degenerate. In fact, we have

$$\begin{aligned}
&\nabla v_g\cdot\mathbf{r}_g^0\equiv 0, \qquad \nabla(v_g\pm c_g)\cdot\mathbf{r}_g^{\pm}=\pm\frac{1}{\rho_g}\frac{\partial}{\partial\rho_g}(\rho_g c_g),\\
&\nabla v_s\cdot\mathbf{r}_s^0\equiv 0, \qquad \nabla(v_s\pm c_s)\cdot\mathbf{r}_s^{\pm}=\pm\frac{1}{\rho_s}\frac{\partial}{\partial\rho_s}(\rho_s c_s),\\
&\nabla v_s\cdot\mathbf{r}_s^c\equiv 0.
\end{aligned} \tag{3.5}$$

Thus, the wave fields are genuinely nonlinear provided that $\dfrac{\partial}{\partial\rho_a}(\rho_a c_a)\neq 0$. This is precisely the same condition encountered in one-phase gas dynamics and can be related to $\left(\dfrac{\partial^2 p_a}{\partial V_a^2}\right)_{\eta_a,\phi_a}$ by the identity

$$\left(\frac{\partial^2 p_a}{\partial V_a^2}\right)_{\eta_a,\phi_a}=2\rho_a^3 c_a\left(\frac{\partial}{\partial\rho_a}(\rho_a c_a)\right)_{\eta_a,\phi_a}.$$

Therefore, we make the following thermodynamic assumptions about the phases:

$$\begin{aligned}
&\left(\frac{\partial p_a}{\partial V_a}\right)_{\eta_a,\phi_a}<0,\\
&\left(\frac{\partial p_a}{\partial \eta_a}\right)_{V_a,\phi_a}>0,\\
&\left(\frac{\partial^2 p_a}{\partial V_a^2}\right)_{\eta_a,\phi_a}>0,
\end{aligned} \tag{3.6}$$

for $a=s,g$. These are the standard convexity assumptions considered in one-phase gas dynamics [13]. These convexity conditions are satisfied by many equations of state, including ideal gases and the equations of state for the solid and gas phases employed in the reactive multiphase flow studies described in [3]. In addition, the conditions in (3.6) guarantee that the Hugoniot curve and the Rayleigh line intersect in at most two points [13], a fact that will be exploited in the last section when we discuss special discontinuous solutions of the multiphase flow equations.

Next we consider the construction of the *generalized Riemann invariants* associated with the various wave fields of the multiphase flow equations. The construction of simple waves outlined in (3.3)–(3.4) involves the solution of the ODE system (3.3) in R^n. One way to construct that curve is to find $n-1$ first integrals for the ODE, that is, functions $\psi_{kj}(\mathbf{U})$, $j=1,\ldots,n-1$ such that

$$\frac{d}{d\sigma}\psi_{kj}(\mathbf{U}_\kappa(\sigma)) = \nabla\psi_{kj}(\mathbf{U}_k(\sigma))\cdot\mathbf{r}_k(\mathbf{U}_k(\sigma)) \equiv 0.$$

Functions $\psi(\mathbf{U})$ that satisfy the PDE

$$\nabla\psi(\mathbf{U})\cdot\mathbf{r}_k(\mathbf{U}) \equiv 0 \tag{3.7}$$

are called generalized Riemann invariants. Therefore to solve (3.3) we need to determine $n-1$ functionally independent invariants in (3.7). In the derivation of the Riemann invariants for the reactive multiphase equations we utilize knowledge about the invariants for one-phase gas dynamics. We will first discuss the invariants away from resonances, i.e. for the case where all the eigenvalues are distinct, and then make some remarks for the case of coalescing eigenvalues. For one-phase gas dynamics the Riemann invariants are well known [14]: in the state variables ρ, v, η, the gas acoustic modes have right eigenvectors $\mathbf{r}^\pm = (1, \pm c/\rho, 0)^T$. Hence the Riemann invariants $\psi^\pm$ solve the PDE

$$\frac{\partial\psi^\pm}{\partial\rho} \pm \frac{c}{\rho}\frac{\partial\psi^\pm}{\partial v} = 0,$$

and two independent solutions are given by

$$\psi_1^\pm = \eta,$$

$$\psi_2^\pm = v \mp \int^\rho \tilde{\rho}^{-1} c(\tilde{\rho},\eta)\, d\tilde{\rho}.$$

The entropy mode has right eigenvector $\mathbf{r}^0 = \left(1, 0, -\frac{c^2}{\rho\Gamma T}\right)^T$ and the Riemann invariant ψ^0 solves the PDE

$$\frac{\partial\psi^0}{\partial\rho} - \frac{c^2}{\rho\Gamma T}\frac{\partial\psi^0}{\partial\eta} = 0,$$

so that two independent solutions are

$$\psi_1^0 = v,$$

$$\psi_2^0 = p.$$

Now we are ready to construct the generalized Riemann invariants for the multiphase flow equations. Since (2.20) shows that the acoustic and entropy right eigenvectors in both phases are essentially the same as in one-phase gas dynamics, then it follows that the Riemann invariants $\psi_a^\pm$ for the acoustic

fields, and the entropy invariants ψ_a^0 satisfy the same PDE as in one-phase gas dynamics

$$\begin{aligned} 0 = \nabla\psi_a^{\pm} \cdot \mathbf{r}_a^{\pm} &= \frac{\partial\psi_a^{\pm}}{\partial\rho_a} \pm \frac{c_a}{\rho_a}\frac{\partial\psi_a^{\pm}}{\partial v_a}, \\ 0 = \nabla\psi_a^{0} \cdot \mathbf{r}_a^{0} &= \frac{\partial\psi_a^{0}}{\partial\rho_a} - \frac{c_a^2}{\rho_a\Gamma_a T_a}\frac{\partial\psi_a^{0}}{\partial\eta_a}, \end{aligned} \tag{3.8}$$

for $a = s, g$. First we consider the acoustic and gas entropy modes because they are associated with only one eigenvector. Since (3.8) involves only one of the phases, it is is clear that the variables for the other phase and the solid volume fraction provide four independent Riemann invariants. Since the PDE determines two additional independent invariants, we have computed all six invariants for the acoustic and gas entropy modes:

Gas acoustic invariants

$$\begin{aligned} \psi_{g1}^{\pm} &= \eta_g, \\ \psi_{g2}^{\pm} &= v_g \mp \int^{\rho_g} \tilde{\rho}^{-1} c_g(\tilde{\rho}, \eta_g)\, d\tilde{\rho}, \\ \psi_{g3}^{\pm} &= \phi_s, \\ \psi_{g4}^{\pm} &= \rho_s, \\ \psi_{g5}^{\pm} &= v_s, \\ \psi_{g6}^{\pm} &= \eta_s, \end{aligned} \tag{3.9}$$

Gas entropy invariants

$$\begin{aligned} \psi_{g1}^{0} &= v_g, \\ \psi_{g2}^{0} &= p_g, \\ \psi_{g3}^{0} &= \phi_s, \\ \psi_{g4}^{0} &= \rho_s, \\ \psi_{g5}^{0} &= v_s, \\ \psi_{g6}^{0} &= \eta_s, \end{aligned} \tag{3.10}$$

Solid acoustic invariants

$$\begin{aligned} \psi_{s1}^{\pm} &= \eta_s, \\ \psi_{s2}^{\pm} &= v_s \mp \int^{\rho_s} \tilde{\rho}^{-1} c_s(\tilde{\rho}, \eta_s)\, d\tilde{\rho}, \\ \psi_{s3}^{\pm} &= \phi_s, \\ \psi_{s4}^{\pm} &= \rho_g, \\ \psi_{s5}^{\pm} &= v_g, \\ \psi_{s6}^{\pm} &= \eta_g, \end{aligned} \tag{3.11}$$

The situation regarding the invariants associated with solid particle speed v_s is more complicated. Since v_s is a double eigenvalue the choice of the eigenvectors $\mathbf{r}_s^0$ and $\mathbf{r}_s^c$ is somewhat arbitrary. Therefore, the invariants associated with $\lambda_s^0 = v_s$ are first integrals of (3.3) for both choices of $\mathbf{r}_s^0$ or $\mathbf{r}_s^c$. Thus the Riemann invariant ψ_s^0 must solve a *system* of two PDE's

$$\begin{aligned} &\nabla\psi_s^0 \cdot \mathbf{r}_s^0 = 0, \\ &\nabla\psi_s^0 \cdot \mathbf{r}_s^c = 0, \end{aligned} \tag{3.12}$$

and therefore we expect in this case to find five independent invariants instead of six. In order to solve (3.12) it is convenient to use the new state variables

$$\tilde{\mathbf{U}} = (\rho_s, v_s, p_s, \phi_s, \rho_g, v_g, \eta_g)^T \tag{3.13}$$

instead of $\mathbf{U}$ given in (2.13). The eigenvalues, eigenvectors, and invariants in the new and old variables satisfy thed following relations:

$$\tilde{\lambda}_k(\tilde{\mathbf{U}}) = \lambda_k(\mathbf{U}),$$

$$\tilde{\mathbf{r}}_k(\tilde{\mathbf{U}}) = \nabla\tilde{\mathbf{U}}(\mathbf{U})\,\mathbf{r}_k(\mathbf{U}),$$

$$\tilde{\psi}(\tilde{\mathbf{U}}) = \psi(\mathbf{U}).$$

The reason for using the change of variables in (3.13) is to simplify the formulas for right eigenvectors associated with the solid particle speed field. In fact, with the change of variables in (3.13), the right eigenvectors $\mathbf{r}_s^0$, $\mathbf{r}_s^c$ in (2.20) reduce to the simpler form

$$\begin{aligned} \tilde{\mathbf{r}}_s^0 &= \frac{\partial\tilde{\mathbf{U}}}{\partial\mathbf{U}}\mathbf{r}_s^0 = (1,0,0,0,0,0,0)^T \\ \tilde{\mathbf{r}}_s^c &= \frac{\partial\tilde{\mathbf{U}}}{\partial\mathbf{U}}\mathbf{r}_s^c = \left(0,0,-\frac{(p_s-p_g)}{\phi_s},1,\frac{\rho_g(v_s-v_g)^2}{\phi_g[(v_s-v_g)^2-c_g^2]},\right. \\ &\qquad \left.\frac{c_g^2(v_s-v_g)}{\phi_g[(v_s-v_g)^2-c_g^2]},0\right)^T, \end{aligned} \tag{3.14}$$

and the linear system of PDE's (3.12) becomes

$$0 = \nabla\tilde{\psi}_s^0 \cdot \tilde{\mathbf{r}}_s^0 = \frac{\partial\tilde{\psi}_s^0}{\partial\rho_s},$$

$$\begin{aligned} 0 = \nabla\tilde{\psi}_s^0 \cdot \tilde{\mathbf{r}}_s^c = &-\frac{p_s-p_g}{\phi_s}\frac{\partial\tilde{\psi}_s^0}{\partial p_s} + \frac{\partial\tilde{\psi}_s^0}{\partial\phi_s} \\ &+ \frac{\rho_g(v_s-v_g)^2}{\phi_g[(v_s-v_g)^2-c_g^2]}\frac{\partial\tilde{\psi}_s^0}{\partial\rho_g} + \frac{\rho_g^2(v_s-v_g)}{\phi_g[(v_s-v_g)^2-c_g^2]}\frac{\partial\tilde{\psi}_s^0}{\partial v_g}. \end{aligned}$$

The first equation simply expresses the fact that $\tilde{\psi}_s^0$ is independent of ρ_s. To investigate the second equation consider its associated equation of

characteristics (which is (3.3) for $\tilde{\mathbf{r}}_s^0$):

$$\frac{dp_s}{dt} = -\frac{(p_s - p_g)}{\phi_s},$$

$$\frac{dv_s}{dt} = 0,$$

$$\frac{d\phi_s}{dt} = 1,$$

$$\frac{d\rho_g}{dt} = \frac{\rho_g (v_s - v_g)^2}{\phi_g [(v_s - v_g)^2 - c_g^2]}, \tag{3.15}$$

$$\frac{dv_g}{dt} = \frac{c_g^2 (v_s - v_g)}{\phi_g [(v_s - v_g)^2 - c_g^2]},$$

$$\frac{d\eta_g}{dt} = 0.$$

The equations for v_s and η_g in (3.15) immediately give two invariants

$$\tilde{\psi}_{s1}^0 = v_s,$$

$$\tilde{\psi}_{s2}^0 = \eta_g,$$

Also, using (3.15) we can derive the following equations for the gas pressure and enthalpy (recall $\beta_g = 0$):

$$\frac{dp_g}{dt} = \frac{\rho_g c_g^2 (v_s - v_g)^2}{\phi_g [(v_s - v_g)^2 - c_g^2]},$$

$$\frac{dh_g}{dt} = \frac{c_g^2 (v_s - v_g)^2}{\phi_g [(v_s - v_g)^2 - c_g^2]}. \tag{3.16}$$

Combining (3.15) and (3.16) it is readily verified that

$$\frac{d}{dt} (\phi_g \rho_g (v_s - v_g)) = 0,$$

$$\frac{d}{dt} (\phi_s p_s + \phi_g p_g + \phi_g \rho_g (v_s - v_g)^2) = 0,$$

$$\frac{d}{dt} (h_g + (v_s - v_g)^2/2) = 0.$$

Consequently, we have the

Solid particle speed invariants

$$\tilde{\psi}^0_{s1} = v_s,$$

$$\tilde{\psi}^0_{s2} = \eta_g,$$

$$\tilde{\psi}^0_{s3} = \phi_g \rho_g (v_s - v_g), \tag{3.17}$$

$$\tilde{\psi}^0_{s4} = \phi_s p_s + \phi_g p_g + \phi_g \rho_g (v_s - v_g)^2,$$

$$\tilde{\psi}^0_{s5} = (v_s - v_g)^2/2 + h_g.$$

It is known that the Riemann invariants associated with a linearly degenerate wave field represent conserved quantities across contact discontinuities. From (3.17) it follows that the particle speed of the solid and the gas entropy are conserved across a contact discontinuity for the solid phase. The remaining three invariants in (3.17) guarantee conservation of mass, momentum, and energy for the *mixture* across the contact discontinuity.

We end this section with some comments regarding the behavior of the Riemann invariants for regions where different eigenvalues coalesce. Again we look at the cases mentioned in Section 2, with emphasis on the choked-flow state. In the cases when $v_s = v_g$, $v_s \pm c_s = v_g$ or $v_s \pm c_s = v_g \pm c_g$ we already know that the corresponding eigenvectors remain independent and the Riemann invariants cannot satisfy the orthogonality condition (3.7) for both eigenvectors. On the other hand, for the case $v_s = v_g \pm c_g$ corresponding to choked flow, the eigenvectors $\mathbf{r}^c_s$ and $\mathbf{r}^{\pm}_g$ do align and the Riemann invariants in (3.17) continue to satisfy (3.7). Moreover, the Riemann invariants (3.17) are still independent of the sonic state. In fact, the Jacobian matrix $\mathbf{J} = \left(\frac{\partial \tilde{\psi}^o_{si}}{\partial \mathbf{U}_j}\right)_{5\times 7}$ with $\mathbf{U}$ given by (2.13) and $\tilde{\psi}^o_{si}$ by (3.17) is

$$\begin{pmatrix} 0 & 1 & 0 & 0 & 0 & 0 & 0 \\ 0 & 0 & 0 & 0 & 0 & 0 & 1 \\ 0 & \phi_g \rho_g & 0 & -\rho_g v_{sg} & \phi_g v_{sg} & -\phi_g \rho_g & 0 \\ \phi_s c_s^2 & 2\phi_g \rho_g v_{sg} & \phi_s \rho_s \Gamma_s T_s & p_{sg} - \rho_g v_{sg}^2 & \phi_g (c_g^2 + v_{sg}^2) & -2\phi_g \rho_g v_{sg} & \phi_g \rho_g \Gamma_g T_g \\ 0 & v_{sg} & 0 & 0 & 2c_g^2/\rho_g & -v_{sg} & (1+\Gamma_g) T_g \end{pmatrix} \tag{3.18}$$

which has full rank even at choked flow points. (Here we have simplified notation using $v_{sg} = v_s - v_g$ and $p_{sg} = p_s - p_g$).

4 Centered rarefaction waves and contact discontinuities

Next we consider some special simple wave solutions of the system. The first solutions are the *centered rarefaction* waves for genuinely nonlinear fields. They are solutions depending on the ratio x/t and can be obtained as the limit of globally smooth solutions. The second type are the *contact discontinuities* for linearly degenerate fields. They are discontinuous solutions depending on the ratio x/t, and are also obtained as limits of globally smooth solutions.

4.1 Centered rarefaction waves for genuinely nonlinear fields

To construct these solutions, it is assumed the k-th field is genuinely nonlinear and $\mathbf{r}_k$ is normalized so that $\nabla\lambda_k \cdot \mathbf{r}_k \equiv 1$. This has the advantage that since $\frac{d}{d\sigma}\lambda_k(\mathbf{U}_k(\sigma)) \equiv \nabla\lambda_k \cdot \mathbf{r}_k \equiv 1$, the wave speed λ_k itself can be chosen as a parameter and (3.3)–(3.4) reduce the computation of $\mathbf{U}(x,t) = \mathbf{U}_k(\lambda_k(x,t))$, where $\mathbf{U}_k$ and λ_k satisfy

$$\begin{aligned} &\frac{d\mathbf{U}_k}{d\lambda_k} = \mathbf{r}_k(\mathbf{U}_k), \\ &\frac{\partial\lambda_k}{\partial t} + \lambda_k\frac{\partial\lambda_k}{\partial x} = 0. \end{aligned} \tag{4.1}$$

The centered rarefaction waves are constructed as follows. Assume $\mathbf{U}_L$ and $\mathbf{U}_R$ are connected by the solution $\mathbf{U} = \mathbf{U}_k(\lambda_k)$ in (4.1) obtained from the Riemann invariants and satisfying $\mathbf{U}_L = \mathbf{U}_k(\lambda_{kL})$, $\mathbf{U}_R = \mathbf{U}_k(\lambda_{kR})$, with $\lambda_{kL} < \lambda_{kR}$. Then the centered rarefaction wave connecting $\mathbf{U}_L$ and $\mathbf{U}_R$ is obtained from the solution of (4.1) with the initial data

$$\lambda_k(x,0) = \begin{cases} \lambda_{kL} & x < 0, \\ \lambda_{kR} & x > 0. \end{cases}$$

This solution is given by $\mathbf{U} = \mathbf{U}_k(\lambda_k(x,t))$, with λ_k defined by

$$\lambda_k(x,t) = \begin{cases} \lambda_{kL} & \text{if } \dfrac{x}{t} < \lambda_{kL}, \\ \dfrac{x}{t} & \text{if } \lambda_{kL} < \dfrac{x}{t} < \lambda_{kR}, \\ \lambda_{kR} & \text{if } \lambda_{kR} < \dfrac{x}{t} \end{cases}$$

Next, consider the case of one-phase gas dynamics. The genuinely nonlinear fields are associated with $\lambda^{\pm} = v \pm c$. In this case it is convenient to rescale $\mathbf{r}^{\pm}$ so that

$$\mathbf{r}^{\pm} = \left(\frac{\partial(\rho c)}{\partial\rho}\right)^{-1}(\pm\rho, c, 0)^T,$$

for then we have $\nabla\lambda^{\pm}\cdot\mathbf{r}^{\pm}\equiv 1$. The Riemann invariants for the gas acoustic determine the velocity and the entropy

$$\eta^{\pm}=\eta_L,$$

$$v^{\pm}=v_L\pm\int_{\rho_L}^{\rho^{\pm}}\rho^{-1}c(\rho,\eta_L)\,d\rho.$$

However, we now have $v^{\pm}$ given in terms of $\rho^{\pm}$ rather than x and t. To determine $\rho^{\pm}$ using $\lambda^{\pm}$, and hence in terms of x,t, we integrate the equation for $\rho^{\pm}$ in (4.1) and obtain

$$\lambda_L\pm\int_{\rho_L}^{\rho^{\pm}}\rho^{-1}\frac{\partial}{\partial\rho}(\rho c)\,d\rho=\lambda^{\pm}.$$

Notice that this last equation, although implicit, provides a unique solution $\rho^{\pm}$ in terms of $\lambda^{\pm}$ because the convexity assumption $\dfrac{\partial}{\partial\rho}(\rho c)>0$ guarantees that $\lambda^{\pm}$ is a monotonic function of $\rho^{\pm}$. In conclusion, the centered rarefaction waves associated with $\lambda^{\pm}=v\pm c$ are given by

$$\begin{aligned}
&\eta^{\pm}=\eta_L,\\
&v^{\pm}=v_L\pm\int_{\rho_L}^{\rho^{\pm}}\rho^{-1}c\,d\rho,\\
&\lambda^{\pm}=\lambda_L\pm\int_{\rho_L}^{\rho^{\pm}}\rho^{-1}\frac{\partial}{\partial\rho}(\rho c)\,d\rho,
\end{aligned}\tag{4.2}$$

with

$$\lambda^{\pm}(x,t)=\begin{cases}\lambda_L & \text{if } \dfrac{x}{t}<\lambda_L,\\[2mm] \dfrac{x}{t} & \text{if } \lambda_L<\dfrac{x}{t}<\lambda_R,\\[2mm] \lambda_R & \text{if } \lambda_R<\dfrac{x}{t}\end{cases}\tag{4.3}$$

Equations (4.2)–(4.3) immediately lead to the construction of centered rarefaction waves for the multiphase system:

Gas acoustic rarefaction waves

$$\begin{aligned}
&\eta_a^{\pm}=\eta_{aL},\\
&v_a^{\pm}=v_{aL}\pm\int_{\rho_{aL}}^{\rho_a^{\pm}}\rho^{-1}c_a\,d\rho,\\
&\lambda_a^{\pm}=\lambda_{aL}\pm\int_{\rho_{aL}}^{\rho_a^{\pm}}\rho^{-1}\frac{\partial}{\partial\rho}(\rho c_a)\,d\rho,
\end{aligned}\tag{4.4}$$

$$\phi_a^{\pm} = \phi_{aL},$$

$$\rho_b^{\pm} = \rho_{bL},$$

$$v_b^{\pm} = v_{bL},$$

$$\eta_b^{\pm} = \eta_{bL},$$

where $a = s, g$, and $b = s$ if $a = g$ and vice-versa. The wave speed $\lambda_a^{\pm}$ is given by (4.3)

$$\lambda_a^{\pm}(x,t) = \begin{cases} \lambda_{aL} & \text{if } \dfrac{x}{t} < \lambda_{aR}, \\ \dfrac{x}{t} & \text{if } \lambda_{aL} < \dfrac{x}{t} < \lambda_{aR}, \\ \lambda_{aR} & \text{if } \lambda_{aR} < \dfrac{x}{t}. \end{cases} \tag{4.5}$$

With the wave speed field given by (4.5), we can solve (4.4) for the density $\rho_a^{\pm}$. Once $\rho_a^{\pm}$ is computed, $v_a^{\pm}$ is determined from (4.4) by integration. The remaining states variables are constant in x and t.

4.2 Contact discontinuities for linearly degenerate fields

To construct these solutions, we assume that the k-th wave field is linearly degenerate: $\nabla\lambda_k \cdot \mathbf{r}_k \equiv 0$. This implies that the speed of propagation $\lambda_k(\mathbf{U}_k(\sigma))$ for the simple wave in (3.2) is constant. Next assume that $\mathbf{U}_L$ and $\mathbf{U}_R$ are connected through the solution of (3.3) with $\mathbf{U}_L = \mathbf{U}_k(\sigma_{kL})$ and $\mathbf{U}_R = \mathbf{U}_k(\sigma_{kR})$ (although this assumption is not needed to construct a solution, it is essential in showing that the discontinuous solution is the limit of smooth solutions). The contact discontinuity is then constructed as the solution of (3.3)–(3.4) with the initial data

$$\sigma_k(x,0) = \begin{cases} \sigma_{kL} & \text{if } x < 0, \\ \sigma_{kR} & \text{if } x > 0. \end{cases}$$

Since $\lambda_k(\mathbf{U}_k(\sigma_k)) \equiv \lambda_k(\mathbf{U}_L)$, $\sigma_k(x,t)$ is given by

$$\sigma_k(x,t) = \begin{cases} \sigma_{kL} & \text{if } \dfrac{x}{t} < \lambda_k(\mathbf{U}_L), \\ \sigma_{kR} & \text{if } \dfrac{x}{t} > \lambda_k(\mathbf{U}_L), \end{cases}$$

and therefore, the contact discontinuity is given simply by

$$\mathbf{U}(x,t) = \begin{cases} \mathbf{U}_L & \text{if } \dfrac{x}{t} < \lambda_k(\mathbf{U}_L), \\ \mathbf{U}_R & \text{if } \dfrac{x}{t} > \lambda_k(\mathbf{U}_L). \end{cases} \tag{4.6}$$

The requirement that the states in the left and the right can be connected by a solution of (3.3) guarantees that the contact discontinuity solution $\mathbf{U}(x,t)$ can be obtained as the limit of smooth traveling wave solutions connecting the same end states [15]: let $\sigma(x)$ be any smooth profile whose values are between σ_{kL} and σ_{kR}, and so that $\sigma(x) \equiv \sigma_{kL}$ for $x < -1$, and $\sigma(x) \equiv \sigma_{kR}$ for $x > 1$. Then

$$\mathbf{U}^{\varepsilon}(x,t) = \mathbf{U}_k\left(\sigma\left(\frac{x - \lambda_k(\mathbf{U}_L)}{\varepsilon}\right)\right),$$

is a smooth traveling wave solution and converges to $\mathbf{U}(x,t)$ as $\varepsilon \to 0$.

For the gas particle speed $\lambda_g^0 = v_g$ it is straightforward to determine the associated contact discontinuities. Since the Riemann invariants in (3.10) represent conserved quantities across the contact discontinuity, then in terms of the state variable $\mathbf{U} = (\rho_s, v_s, \eta_s, \phi_s, \rho_g, v_g, p_g)^T$, we have $\mathbf{U}(x,t)$ given by (4.6) with $\lambda_k(\mathbf{U}_L) = v_{gL}$, and $\mathbf{U}_L$, $\mathbf{U}_R$ satisfy

$$\begin{aligned} &\rho_{sR} = \rho_{sL}, \quad v_{sR} = v_{sL}, \quad \eta_{sR} = \eta_{sL}, \quad \phi_{sR} = \phi_{sL}, \\ &\rho_{gR} \neq \rho_{gL}, \quad v_{gR} = v_{gL}, \quad p_{gR} = p_{gL}. \end{aligned} \tag{4.7}$$

Therefore a contact discontinuity moving with the gas speed v_g is simply a discontinuity for the density in the gas phase, just as in one-phase gas dynamics.

On the other hand, the determination of contact discontinuities moving at the solid particle speed is more complicated because v_s is a double eigenvalue. Again, it is convenient to work with the variable $\mathbf{U} = (\rho_s, v_s, p_s, \phi_s, \rho_g, v_g, p_g)^T$ defined in (3.13) (we dropped the for convenience). The Riemann invariants for the solid particle speed are conserved quantities across the contact discontinuity. Therefore, for a given left state $\mathbf{U}_L$, the possible right states $\mathbf{U}_R$ for which a contact discontinuity exists belong to the two dimensional surface in R^7 described by the Riemann invariants in (3.17):

$$\begin{aligned} &v_s = v_{sL}, \\ &\eta_g = \eta_{gL}, \\ &\phi_g \rho_g (v_s - v_g) = \phi_{gL} \rho_{gL} (v_{sL} - v_{gL}) = M, \\ &\phi_s p_s + \phi_g p_g + \phi_g \rho_g (v_s - v_g)^2 = \phi_{sL} p_{sL} + \phi_{gL} p_{gL} + \phi_{gL} \rho_{gL} (v_{sL} - v_{gL})^2 = P, \\ &(v_s - v_g)^2/2 + h_g = (v_{sL} - v_{gL})^2/2 + h_{gL} = E. \end{aligned} \tag{4.8}$$

In addition, we require that the left and right states can be connected by a solution of (3.3), so that the contact discontinuity can be obtained as the limit of smooth traveling waves. Since we are now on a two dimensional surface, it should be possible to reach $\mathbf{U}_R$ from $\mathbf{U}_L$ by following curves defined by (3.3) with right eigenvectors $\mathbf{r}_s^0$ or $\mathbf{r}_s^c$ given by (3.14), or a successive application of both. The curves generated by the right eigenvector $\mathbf{r}_s^0$ are given

by

$$\frac{d\mathbf{U}}{d\sigma} = \mathbf{r}_s^0(\mathbf{U}) = \mathbf{e}_1, \quad \mathbf{U}(0) = \mathbf{U}_L, \tag{4.9}$$

and the solution trajectories are simply straight lines parallel to the ρ_s axis:

$$\begin{aligned} &\rho_s = \rho_{sL} + \sigma, \quad v_s = v_{sL}, \quad p_s = p_{sL}, \quad \phi_s = \phi_{sL}, \\ &\rho_g = \rho_{gL}, \quad v_g = v_{gL}, \quad \eta_g = \eta_{gL}. \end{aligned} \tag{4.10}$$

We denote the solution of (4.9) by $\mathbf{U}^1(\mathbf{U}_L, \sigma)$:

$$\mathbf{U}^1(\mathbf{U}_L, \sigma) = \mathbf{U}_L + \sigma \mathbf{e}_1.$$

Clearly the states connected to $\mathbf{U}_L$ through this solution simply represent discontinuities in the solid density as in one-phase gas dynamics. To study the states that can be connected to $\mathbf{U}_L$ through curves defined by $\mathbf{r}_s^c$ in (3.14), it is convenient to rescale this vector field with the scalar factor $\mu = \phi_g[(v_s - v_g)^2 - c_g^2]$. Then equation (3.3) becomes

$$\frac{d\mathbf{U}}{d\sigma} = \mu \mathbf{r}_s^c(\mathbf{U}), \quad \mathbf{U}(0) = \mathbf{U}_L, \tag{4.11}$$

and componentwise it is given explicitly by

$$\begin{aligned} &\frac{d\rho_s}{d\sigma} = 0, \\ &\frac{dv_s}{d\sigma} = 0, \\ &\frac{dp_s}{d\sigma} = -\phi_g(p_s - p_g)[(v_s - v_g)^2 - c_g^2]/\phi_s, \\ &\frac{d\phi_s}{d\sigma} = \phi_g[(v_s - v_g)^2 - c_g^2], \\ &\frac{d\rho_g}{d\sigma} = \rho_g(v_s - v_g)^2, \\ &\frac{dv_g}{d\sigma} = c_g^2(v_s - v_g), \\ &\frac{d\eta_g}{d\sigma} = 0. \end{aligned} \tag{4.12}$$

Call the solution of (4.11) $\mathbf{U}^2(\mathbf{U}_L, \sigma)$. Notice that (4.12) is essentially the same as (3.15). The Riemann invariants in (3.17) are first integrals of (4.12).

From (4.12) it follows that ρ_s, v_s, and η_g are constant, the last two in agreement with (3.17). It also follows that $v_{sg} = v_s - v_g$ and ρ_g are solutions of the 2×2 autonomous system

$$\begin{aligned} \frac{d\rho_g}{d\sigma} &= \rho_g v_{sg}^2, \\ \frac{dv_{sg}}{d\sigma} &= -c_g^2 v_{sg}. \end{aligned} \tag{4.13}$$

Using (4.13) and the Riemann invariants in (3.17) we can describe the states $\mathbf{U}$ that can be connected to $\mathbf{U}_L$. From (3.17) it is clear that the solution of (4.13) has the gas stagnation enthalpy ψ_{s5}^0 as first integral

$$h_g(\rho_g) + v_{sg}^2/2 = E, \tag{4.14}$$

where the enthalpy $h_g(\rho_g)$ is given by

$$h_g(\rho_g) = \int_0^{\rho_g} \rho^{-1} c_g^2(\rho)\, d\rho.$$

For the remaining of this section we make the further thermodynamic assumption that the equation of state is such that

$$\begin{aligned} &c_g(\rho_g) \to 0, \quad \text{as } \rho_g \to 0, \\ &h_g(\rho_g) \to 0, \quad \text{as } \rho_g \to 0, \\ &h_g(\rho_g) \to \infty, \quad \text{as } \rho_g \to \infty, \end{aligned} \tag{4.15}$$

which is certainly satisfied for ideal gases. Since h_g is an increasing function of ρ_g, (4.14) shows that the maximum value of the gas density is ρ_*, with $h_g(\rho_*) = E$. Also the maximum value of v_{sg} is $\sqrt{2E}$, see Fig. 1. The equili-

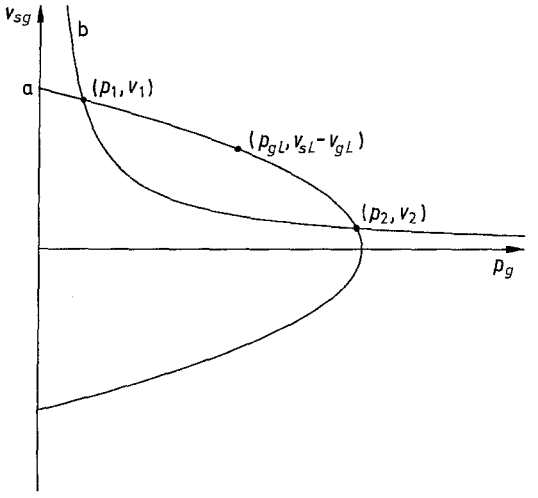

Fig. 1. Plot in the $\rho_g - v_{sg}$ plane showing the energy level curve a: $h_g + v_{sg}^2/2$, and the curve b: $M = \rho_g v_{sg}$

brium points of (4.13) are given by the axes $\rho_g = 0$ and $v_{sg} = 0$. With this information we can determine the points (ρ_g, v_{sg}) that are connected to $(\rho_{gL}, v_s - v_g)$ in (4.13): if $\rho_{gL} > 0$ and $v_{sL} - v_{gL} > 0$ (resp. < 0), then the curve is defined by (4.14) in the quadrant $\rho_g > 0$, $v_{sg} > 0$ (resp. $v_{sg} < 0$). On the other hand, if $\rho_{gL} = 0$ or $v_s - v_g = 0$, then the curve reduces to the point $(\rho_{gL}, v_s - v_g)$.

The volume fraction is determined from the invariant ψ^0_{s3} expressing conservation of mass for the mixture in (3.17) and (4.8):

$$\phi_g = M/[\rho_g v_{sg}].$$

However, the volume fraction has to satisfy the constraint that $0 < \phi_g < 1$, and this further restricts the admissible states to satisfy $\rho_1 < \rho_g < \rho_2$, where ρ_1 and ρ_2 are defined by the points of intersection of the hyperbola $v_{sg}\rho_g = M$ and the curve (4.14) (see Fig. 1)

$$h_g(\rho_g) + M^2/[2\rho_g^2] = E. \tag{4.16}$$

Finally, the solid phase pressure is computed from the invariant ψ^0_{s4} expressing conservation of momentum for the mixture in (3.17) and (4.8):

$$p_s = \phi_s^{-1}[P - \phi_g p_g - \phi_g \rho_g (v_s - v_g)^2].$$

Next, we can connect other points to $\mathbf{U}_L$ by successively using the solutions $\mathbf{U}^1(\mathbf{U}_0, \sigma_1)$ and $\mathbf{U}^2(\mathbf{U}_0, \sigma_2)$ previously discussed. Notice that these solution trajectories are orthogonal because the corresponding tangent vectors $\mathbf{r}^0_s$ and $\mathbf{r}^c_s$ in (3.14) are orthogonal. Also, since $\mathbf{r}^c_s(\mathbf{U})$ does not depend on the variable ρ_s, the solution $\mathbf{U}^2$ of (4.11) with data translated in the ρ_s direction is obtained by translating the solution by the same amount in the ρ_s direction with nontranslated data, that is,

$$\mathbf{U}^2(\mathbf{U}_0 + \sigma_1 \mathbf{e}_1, \sigma_2) = \mathbf{U}^2(\mathbf{U}_0, \sigma_2) + \sigma_1 \mathbf{e}_1.$$

But this implies that the solutions $\mathbf{U}^1$ and $\mathbf{U}^2$ commute:

$$\begin{aligned}\mathbf{U}^2(\mathbf{U}^1(\mathbf{U}_0, \sigma_1), \sigma_2) &= \mathbf{U}^2(\mathbf{U}_0 + \sigma_1 \mathbf{e}_1, \sigma_2). \\ &= \mathbf{U}^2(\mathbf{U}_0, \sigma_2) + \sigma_1 \mathbf{e}_1 \\ &= \mathbf{U}^1(\mathbf{U}^2(\mathbf{U}_0, \sigma_2), \sigma_1),\end{aligned}$$

and this commutation property shows that points in the two dimensional surface can be connected to $\mathbf{U}_L$ by using trajectories generated by $\mathbf{r}^0_s$ and $\mathbf{r}^c_s$ in either order; if $\mathbf{U}_R$ is connected to $\mathbf{U}_L$ by first applying the solution $\mathbf{U}^1$ and then the solution $\mathbf{U}^2$, then it follows from the commutation property that the connection can be done in the reverse order, first by applying $\mathbf{U}^2$, and then the solution $\mathbf{U}^1$. This analysis also shows that the set of points that can be connected to $\mathbf{U}_L$ forms a two dimensional ruled surface with generators parallel to the ρ_s axis, and generated by the solution curve $\mathbf{U}^2(\mathbf{U}_L, \sigma_2)$.

Now we can collect the results of this analysis and determine all the states $\mathbf{U}_R$ that can be connected to $\mathbf{U}_L$, and therefore the contact discontinuities propagating at the solid particle speed. The answer depends on whether

$v_{sL} - v_{gL}$ vanishes or not; for two admissible states $\mathbf{U}_L$ and $\mathbf{U}_R$, the contact discontinuity is given by (4.6) with $\lambda_k(\mathbf{U}_L) = v_{sL}$, and the admissible state $\mathbf{U}_R$ is prescribed as follows:
a) If $v_{sL} - v_{gL} = 0$, then the states $\mathbf{U}_R$ that can be connected to $\mathbf{U}_L$ are given by

$$\rho_{sR} > 0, \quad v_{sR} = v_{sL}, \quad p_{sR} = {}_{sL}, \quad \phi_{sR} = \phi_{sL},$$

$$\rho_{gR} = \rho_{gL}, \quad v_{gR} = v_{sL}, \quad p_{gR} = p_{gL}. \tag{4.17}$$

and ρ_{sR} is arbitrary, so that in this case we have only a density discontinuity in the solid phase, analogous to the contact discontinuities in one-phase gas dynamics. On the other hand,
b) If $v_{sL} - v_{gL} \neq 0$, then the states $\mathbf{U}_R$ that can be connected to $\mathbf{U}_L$ are given by

$$\begin{aligned}
&\rho_{sR} > 0, \\
&v_{sR} = v_{sL}, \\
&p_{sR} = \phi_{sR}^{-1}[P - \phi_{gR}p_{gR} + \phi_{gR}\rho_{gR}(v_{sR} - v_{gR})^2], \\
&\phi_{sR} = 1 - \phi_{gR}, \\
&0 < \rho_1 < \rho_{gR} < \rho_2, \\
&v_{gR} = v_{sR} + \operatorname{sign}(v_{gL} - v_{sL})\,[2(E - h_g(\rho_{gR}, \eta_{gR}))]^{1/2}, \\
&\eta_{gR} = \eta_{gL}, \\
&\phi_{gR} = M/(\rho_{gR}v_{gR}),
\end{aligned} \tag{4.18}$$

where ρ_1 and ρ_2 are the two positive solutions of (4.16). Therefore, (4.18) completely characterizes the two dimensional surface of the states $\mathbf{U}_R$ that can be connected to $\mathbf{U}_L$, and this surface is explicitly parametrized in terms of the densities ρ_{sR} and ρ_{gR} for the solid and the gas phases, repectively. Finally, we remark that the six dimensional surface of choked flow states

$$(v_s - v_g)^2 = c_g^2 \tag{4.19}$$

intersects the two dimensional surface defined by the Riemann invariants in (4.8) at exactly two lines parallel to the ρ_s axis, one line being in each of the regions $v_s > v_g$ and $v_s < v_g$. First we determine the gas density. From (4.19) and the conservation of stagnation enthalpy for the gas phase (4.8), we obtain

$$h_g(\rho_g, \eta_g) + c_g^2(\rho_g, \eta_g)/2 = E. \tag{4.20}$$

The left side of (4.20) defines an increasing function of ρ_g (η_g is constant) as consequence of the convexity assumption (3.6)

$$\frac{\partial}{\partial \rho_g}(h_g + c_g^2/2) = \frac{c_g}{\rho_g}\frac{\partial}{\partial \rho_g}(\rho_g c_g) > 0,$$

and because of the additional assumption (4.15) about the equation of state we have that $h_g + c_g^2/2$ goes to zero when ρ_g goes to zero, and it goes to infinity when ρ_g goes to infinity. This implies that there is a unique solution ρ_g^* of (4.20). Now we can determine two values for v_g from (4.19) and the fact that $v_s = v_{sL}$ in (4.8), that is,

$$v_g = v_{sL} \pm c_g^2(\rho_g^*, \eta_{gL}) .$$

The remaining state variables p_s, ϕ_s, and η_g can then be determined from (4.8), and ρ_s is arbitrary. This proves the remark.

5 Special discontinuous solutions of the multiphase flow equations

After discussing centered rarefaction waves and contact discontinuities, the next logical step is to investigate shock wave discontinuities for the multiphase flow system. However, as we will shortly see, there are problems in determining the jump conditions in the multiphase flow system because it is not in *divergence form.* This loss in the divergence form structure is due to the presence of solid volume fraction spatial derivatives in the momentum and energy equations for each phase, that is $p_g \dfrac{\partial \phi_a}{\partial x}$ and $v_g p_s \dfrac{\partial \phi_a}{\partial x}$. Technically, one of the main difficulties in studying discontinuous solutions of equations that are not in divergence form is how to define the product of two distributions, and currently there exists no complete theory for discontinuous distribution solutions of non-strictly hyperbolic, non-conservation form hyperbolic systems such as the multiphase flow system considered here. According to (2.7), the solid volume fraction is transported at the solid particle speed v_s, so it is plausible that for discontinuities moving at speeds different from the solid particle speed there is no problem in formulating the jump conditions. This will prove to be the case, for we will show below that in this case the volume fraction remains continuous across the shock. The problem of determining all the possible shock states in the case where the shock moves at the particle speed remains open. Here we will consider only the jump conditions for shocks moving at the solid speed v_s *only* for the case where the solid volume fraction does not jump across the shock, and therefore we avoid the technical problem of dealing with products of distributions. Although this is a special case, it is interesting. In fact, in this case we can construct two different discontinuous solutions with the same upstrem conditions, provided that the velocity of the gas relative to the solid is supersonic. A deeper study of shocks moving at the solid particle velocity and with jumps in the volume fraction across the shock requires the inclusion of diffusive transport mechanisms within the shock layer and will be the subject of future study.

For the study of discontinuous solutions we recast the multiphase flow equations (2.1)–(2.7) into the *conservation* form ($a = s, g$)

Conservation of mass

$$\frac{\partial}{\partial t}(\phi_a \rho_a) + \frac{\partial}{\partial x}(\phi_a \rho_a v_a) = C_a^\dagger$$

Conservation of momentum

$$\frac{\partial}{\partial t}(\phi_a \rho_a v_a) + \frac{\partial}{\partial x}(\phi_a \rho_a v_a^2 + \phi_a p_a) - p_g \frac{\partial \phi_a}{\partial x} = m_a^\dagger \tag{5.1}$$

Conservation of energy

$$\frac{\partial}{\partial t}(\phi_a \rho_a E_a) + \frac{\partial}{\partial x}\left((\phi_a \rho_a E_a + \phi_a p_a) v_a + q_a\right) - p_g v_s \frac{\partial \phi_a}{\partial x} = e_a^\dagger$$

Solid mass density

$$\frac{\partial \rho_s}{\partial t} + \frac{\partial}{\partial x}(\rho_s v_s) = -\frac{\rho_s}{\phi_s} F,$$

where $E_a = e_a + v_a^2/2$ is the total energy of the a phase. As for one-phase flows, a change of variables calculation using (2.11) shows that for smooth solutions the systems (2.1)–(2.7) and (5.1) are equivalent. In addition, the solid mass density equation (5.1) is a direct consequence of combining the conservation of mass equation (2.1) and the solid volume fraction equation (2.7).

The phase interaction terms are given by

$$C_s^\dagger = -C_g^\dagger,$$

$$m_s^\dagger = -m_g^\dagger = -\left(\delta + \frac{C_s^\dagger}{2}\right)(v_s - v_g) + C_s^\dagger v_s,$$

$$e_s^\dagger = -e_g^\dagger = -\left(\delta + \frac{C_s^\dagger}{2}\right)(v_s - v_g) v_s - (p_s - \beta_s) F \tag{5.2}$$

$$-h(T_s - T_g) + E_s C_s^\dagger,$$

$$q_a = -k_a \frac{\partial T_a}{\partial x},$$

Additionally, for discontinuous solutions, the system (5.1) is supplemented by the entropy inequality for the mixture [3]

$$\sum_a \left[\phi_a \rho_a \left(\frac{\partial \eta_a}{\partial t} + v_a \frac{\partial \eta_a}{\partial x}\right) + \eta_a C_a^\dagger + \frac{\partial}{\partial x}\left(\frac{q_a}{T_a}\right)\right] \geqq 0.$$

We discard the heat conduction term in the entropy inequality and use the conservation of mass equation (5.1) to recast the entropy inequality as

$$\frac{\partial}{\partial t}\left(\sum_a \phi_a \rho_a \eta_a\right) + \frac{\partial}{\partial x}\left(\sum_a \phi_a \rho_a \eta_a v_a\right) \geqq 0. \tag{5.3}$$

The system (5.1) is not in divergence form because of the presence of the non-divergence form terms $p_g \frac{\partial \phi_s}{\partial x}$ and $p_g v_s \frac{\partial \phi_s}{\partial x}$ in the momentum and energy equation. However, the conservation equations for the mixture *are* in divergence form

$$\begin{aligned}
&\frac{\partial}{\partial t}\left(\sum_a \phi_a \rho_a\right) + \frac{\partial}{\partial x}\left(\sum_a \phi_a \rho_a v_a\right) = 0,\\
&\frac{\partial}{\partial t}\left(\sum_a \phi_a \rho_a v_a\right) + \frac{\partial}{\partial x}\left(\sum_a (\phi_a \rho_a v_a^2 + \phi_a p_a)\right) = 0.\\
&\frac{\partial}{\partial t}\left(\sum_a \phi_a \rho_a E_a\right) + \frac{\partial}{\partial x}\left(\sum_a [(\phi_a \rho_a E_a + \phi_a p_a)\, v_a + q_a]\right) = 0.
\end{aligned} \tag{5.4}$$

Since the conservation equations for the mixture are in divergence form, the standard derivation of the jump conditions can be applied to these equations [13]. Let $[f]$ denote the difference of the values of f at the right and left of the discontinuity, $[f] = f_L - f_R$, v is the velocity of the discontinuity and $U_a = v_a - v$. Then (5.4) implies the following jump conditions for mass, momentum, and energy for the mixture across the discontinuity

$$\begin{aligned}
&\sum_a [\phi_a \rho_a U_a] = 0,\\
&\sum_a [\phi_a (\rho_a U_a^2 + p_a)] = 0,\\
&\sum_a [\phi_a \rho_a U_a (h_a + U_a^2/2)] = 0.
\end{aligned} \tag{5.5}$$

Similarly, (5.3) implies the jump condition for the entropy of the mixture

$$\sum_a [\phi_a \rho_a \eta_a U_a] = 0. \tag{5.6}$$

The conservation of mass, momentum, and energy for the mixture given in (5.5), as well as the entropy inequality for the mixture in (5.6) must be satisfied by any distribution solution of the multiphase flow system. Notice in particular that the jump conditions given in (4.8) for a contact discontinuity moving at the solid particle velocity do imply the jump conditions for the mixture in (5.5). In addition, the equations of mass conservation and the solid mass density equation (5.1) are also in divergence form, hence we obtain three

additional jump conditions for the phases

$$[\phi_a \rho_a U_a] = 0,$$
$$[\rho_s U_s] = 0. \tag{5.7}$$

Therefore, if $U_s = v_s - v \neq 0$, i.e., if the discontinuity does not travel at the solid particle speed, then (5.7) implies that $[\phi_a] = 0$, and the solid volume fraction does not jump across the discontinuity. In this case the non-divergence form terms in the equations of momentum and energy are classical functions, and the standard derivation of the jump conditions can be applied in this case. The resulting jump conditions for the momentum and energy of each phase are

$$[\phi_a(\rho_a U_a^2 + p_a)] = 0,$$
$$[\phi_a \rho_a U_a(h_a + U_a^2/2)] = 0. \tag{5.8}$$

The jump conditions in (5.6)–(5.8), combined with $[\phi_a] = 0$, yield the jump conditions for a shock not moving at the solid particle speed ($U_s \neq 0$):

$$[\rho_a U_a] = 0,$$
$$[\rho_a U_a^2 + p_a] = 0,$$
$$[\rho_a U_a(h_a + U_a^2/2)] = 0, \tag{5.9}$$
$$[\phi_a] = 0,$$
$$\sum_a [\phi_a \rho_a U_a \eta_a] \geqq 0.$$

The first three equations in (5.9) are the well-known jump conditions for mass, momentum, and energy, and they hold for each phase. Therefore the classical analysis for gas dynamic discontinuities [13] applies here for each phase independently. After the right state U_R has been determined for a given left state U_L and the discontinuity speed v, the entropy inequality for the mixture in (5.9) needs to be verified. Notice that here the entropy may decrease in one of the phases across the discontinuity as long as the mixture entropy does not decrease.

Next we consider the case where $[U_s] = 0$, that is, where $v = v_{sR} = v_{sL}$. In this case (5.7) does not imply that $[\phi_a] = 0$. However, the jump conditions (5.5)–(5.7) must hold for any admissible discontinuous solution, and in this case they reduce to

$$[v_s] = 0,$$
$$[\phi_g \rho_g(v_g - v_s)] = 0,$$
$$[\phi_s p_s + \phi_g p_g + \phi_g \rho_g(v_g - v_s)^2] = 0, \tag{5.10}$$
$$[\phi_g \rho_g(v_g - v_s)\,(h_g + (v_g - v_s)^2/2)] = 0,$$
$$[\phi_g \rho_g(v_g - v_s)\,\eta_g] \geqq 0.$$

Equations (5.10) define a three dimensional manifold for the states variables in R^7. Clearly, the two dimensional surface of contact discontinuity states defined by (4.8) is embedded in this three dimensional manifold. However, since the contact discontinuities satisfy $[\eta_g] = 0$, the entropy of the mixture does not increase across the contact discontinuity and therefore they cannot be considered as shocks. This also shows that the three dimensional manifold defined by (5.10) contains many more points besides shocks. To elucidate which of these points represent shock end states will require a detailed analysis of the shock layer and the various transport mechanisms therein. Here we focus instead on the special but nevertheless interesting case where the discontinuity satisfies $[\phi_s] = 0$. In this case (5.9) reduce to

$$
\begin{aligned}
&[\phi_s] = 0,\\
&[p_s] = 0,\\
&[v_s] = 0,\\
&[\rho_g(v_g - v_{sL})] = 0,\\
&[\rho_g(v_g - v_{sL})^2 + p_g] = 0,\\
&[\rho_g(v_g - v_{sL})\ (h_g + (v_g - v_{sL})^2/2)] = 0,\\
&[\rho_g(v_g - v_{sL})\ \eta_g] \geqq 0.
\end{aligned}
\tag{5.11}
$$

The first three equations for the solid phase in (5.11) imply that there is a contact discontinuity in the solid phase. The remaining four conditions are the gas dynamic jump relations for the gas phase, where the discontinuity is moving at the solid particle speed.

We conclude this section by obtaining some special discontinuous solutions of the multiphase flow system given by (5.11). In these solutions we assume that $v_{gL} - v_{sL} > 0$, and that the upstream end state $\mathbf{U}_L$ is given. The discontinuity moves at speed v_{gL}, and the downstream end state $\mathbf{U}_R$ is determined by (5.11). The determination of the solid phase variables from (5.11) is straightforward. On the other hand, to determine the downstream values of the gas variables we follow the classical analysis for gas dynamic discontinuities given in [13]. The downstream values of the pressure p_g and specific volume V_g for the gas phase are determined by the intersection of the Rayleigh line R given by

$$
p_g - p_{gL} = -m^2(V_g - V_{gL}), \tag{5.12}
$$

where $m = \rho_g(v_{gL} - v_{sL})$, and the Hugoniot curve H, that is

$$
e_g(p_g, V_g) - e_g(p_{gL}, V_{gL}) = -(p_g + p_{gL})\ (V_g - V_{gL})/2. \tag{5.13}
$$

Since the equation of state for the gas phase satisfies the convexity conditions in (3.6), the Rayleigh line (5.12) and the Hugoniot curve (5.13) intersect in at most two points [13]. There are different cases to be considered when determining the downstream values V_{gR} and p_{gR} for the gas variable, and they depend on the value of the upstream *relative Mach number* $M = (v_{gL} - v_{sL})/c_{gL}$ (see Fig. 2):

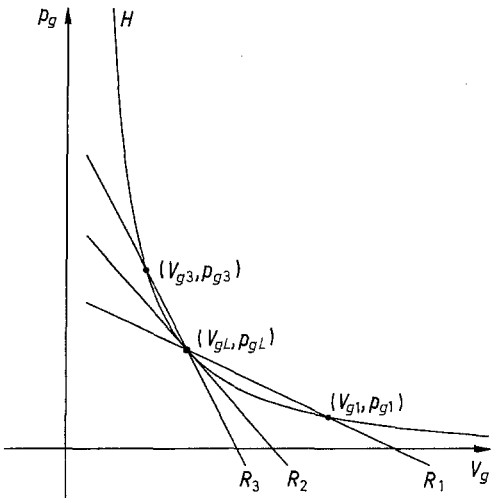

Fig. 2. Plot in the $V_g - p_g$ plane showing the relative position of the Rayleigh line (R) and the Hugoniot curve (H) for the gas phase in the three regimes of the relative Mach number M. Case 1: $M < 1$, $R = R_1$. Case 2: $M = 1$, $R = R_2$. Case 3: $M > 1$, $R = R_3$

Case 1: $M < 1$ (relative subsonic flow). In this case the Rayleigh line R_1 and the Hugoniot curve H intersect at the points (V_{gL}, p_{gL}) and (V_{g1}, p_{g1}) (Fig. 2). The point (V_{gL}, p_{gL}) trivially satisfies the entropy condition in (5.11), but the point (V_{g1}, p_{g1}) violates it [13]. Therefore in this case the upstream and downstream gas phase variables are forced to take on the same values, and the discontinuous solution given by (5.11) reduces to a density discontinuity in the solid phase.

Case 2: $M = 1$ (choked flow case). In this case the Rayleigh line R_2 is tangent to the Hugoniot curve H at the point (V_{gL}, p_{gL}) (Fig. 2). Repeating the analysis above for the subsonic case shows that we get again only a density discontinuity for the solid phase.

Case 3: $M > 1$ (relative supersonic flow). In this case the Rayleigh line R_3 and the Hugoniot curve H intersect at the points (V_{gL}, p_{gL}) and (V_{g3}, p_{g3}) (Fig. 2). In this case the point (V_{g3}, p_{g3}) gives an increase in the entropy of the mixture in (5.11) across the discontinuity. Therefore in this case we have two possible discontinuous solutions of the multiphase flow system with the same upstream values of the state variables and moving at the same speed v_{sL}: the first solution consists of a contact discontinuity for the solid phase where only the solid density changes across the discontinuity, with the downstream end state $\mathbf{U}_R$ given by

$$\mathbf{U}_R = (\rho_{sR}, v_{sL}, p_{sL}, \phi_{sL}, \rho_{gL}, v_{sL} + m/\rho_{gL}, p_{gL})^T, \tag{5.14}$$

just as in the two previous cases. The second solution consists of a contact discontinuity for the solid phase and a shock in the gas phase, and the downstream end state $\mathbf{U}_R$ is obtained by setting V_{g3} and p_{g3} as the downstream values of the specific volume and pressure for the gas

$$\mathbf{U}_R = (\rho_{sR}, v_{sL}, p_{sL}, \phi_{sL}, V_{g3}^{-1}, v_{sL} + mV_{g3}, p_{g3})^T. \tag{5.15}$$

Both solutions satisfy the jump condition for the mixture entropy. For the contact discontinuity there is no increase of entropy across the discontinuity whereas for the shock solution there is. The motion of the gas phase relative to the solid phase changes from supersonic to subsonic in the shock solution, but remains supersonic for the contact discontinuity. Also, both solutions satisfy Lax's geometric shock conditions [12]. For the contact discontinuity solution the v_s characteristic runs along the discontinuity whereas the the remaining characteristics cross it. For the gas-shock solution the discontinuity seperates the $v_g - c_g$ characteristics since $v_{gL} - c_{gL} > v_s > v_{gR} - c_{gR}$, and Lax's geometric shock condition is satisfied because the $v_g - c_g$ impinges on the shock whereas the v_s characteristic runs along the discontinuity and the remaining characteristics cross the discontinuity. Under which conditions either of these solutions is the physically realizable remains the subject of future study.

6 Summary

In this study, we have examined the mathematical character of a multiphase mixture description used to model fully-compressible, nonequilibrium reactive multiphase flows. A characteristic analysis reveals that the system of equations is hyperbolic; however, the description becomes degenerate where the flow is locally sonic. We have determined the left and right eigenvectors for the system of equations and have recast the description in characteristic form. After classifying the wave field, we derived the Riemann invariants and constructed simple wave solutions. Additionally, special discontinuous solutions of the multiphase flow equations have been determined. Having established this mathematical foundation, sufficient framework has been provided towards development of a characteristic-based numerical method.

Acknowledgements: We gratefully acknowledge fruitful discussions with the late J. W. Nunziato (Sandia National Labs), P. Lax (Courant Institute) and A. Majda (Princeton University). Finally, we also thank the reviewers for their help in editing this manuscript.

References

1. Truesdell, C. and R. Toupin: The Classical Field Theories, Handbuch der Physik (Ed. S. Flugge), Vol. II/1, p. 226. Berlin: Springer 1960
2. Truesdell, C.; N. Noll: The Nonlinear Field Theories of Mechanics, Handbuch der Physik (Ed. S. Flugge), Vol. III/3r. Berlin: Springer 1965
3. Baer, M.; Nunziato, J.: A Two-Phase Mixture Theory for the Deflagration-to-Detonation Transition (DDT) in Reactive Granular Materials. Int. J. Multiphase Flow 12 (1986) 861–889
4. Stewart, H.; Wendroff, B.: Two-phase flow: models and methods. J. Comp. Phys. 56 (1984) 363–409

5. Hicks, D.: Well-posedness of the two-phase flow problem, part 2: stability analyses and microstructural models. Report SAND 80-1276, Sandia National Lab.: Albuquerque 1980
6. Embid, P.; Baer, M.: Modeling two-phase flow of reactive granular materials. IMA Volumes Math. Applications 29 (1991) 58–67
7. Embid, P.; Hunter, J.; Majda, A.: Simplified asymptotic equations for the transition to detonation in reactive granular materials. SIAM J. Appl. Math (to appear)
8. Embid, P.; Majda, A.: An asymptotic theory for hot spot formation and transition to detonation for reactive granular materials. Combust. Flame (to appear)
9. Baer, M.; Gross, R.; Nunziato, J.; Igel, E.: An experimental and theoretical study of deflagration-to-detonation transition (DDT) in the granular explosive CP. Combust. Flame 65 (1986) 15–30
10. Baer, M.; Nunziato, J.; Embid, P.: Deflagration to detonation transition in reactive granular materials. Prog. Astronaut. Aeronaut. 135 (1991) 481–512
11. Majda, A.: Compressible Fluid Flow and Systems of Conservation Laws in Several Space Variables. New York: Springer 1984
12. Lax, P.: Hyperbolic System of Conservation Laws II. Comm. Pure Appl. Math.10 (1957) 537–566
13. Courant, R.; Friedrichs, K.: Supersonic Flow and Shock Waves. New York: Springer 1976
14. Jeffrey, A.; Taniuti, T.: Non-Linear Wave Propagation. New York: Academic Press 1964
15. Majda, A.: Theory of Conservation Laws, unpublished notes, Princeton University 1984

P. Embid
Department of Mathematics and Statistics
University of New Mexico
Albuquerque, NM 87131
USA

M. Baer
Fluid and Thermal Sciences Department
Sandia National Laboratories
Albuquerque, NM 87185
USA

Received February 12, 1992